International Journal for Housing Science and Its Applications
Publish August 6, 2025. Volume 46, Issue 3 Pages 4711-4721

https://doi.org/10.70517/ijhsa463403

Mechanisms for Cultural Heritage Preservation and Pathways for Technological Integration in Digital Art Creation

Jiachang Huang[1,*]
[1] School of Art and Design, Wuhan Technology and Business University, Wuhan, Hubei, 430065, China
Corresponding authors: (e-mail: huangjiahexin@163.com).

Abstract In order to realize the integration of digital technology and traditional culture, and to explore the innovation path of digital art while carrying out cultural inheritance, this paper carries out computer-aided creation of Chinese paintings by means of computer-aided creation technology. Comprehensively utilizing the region growth algorithm, line drawing intelligent generation model and digital painting virtual pigment model and other computer-assisted methods for the creation of Chinese paintings, followed by objective and subjective evaluation of the creation effect. The model in this paper has the maximum values of recall, precision, mAP, PSNR, SSIM, and the minimum values of LPIPS and FID on both Scene and People datasets, and the optimal effect is obtained on both datasets. The Chinese paintings created by the method of this paper received an overall subjective evaluation of 4.34, with the scores of the primary indexes exceeding 4.25 and the scores of the secondary indexes not less than 4.15, and the viewers have a better view of the Chinese paintings created by the computer-aided creation method of this paper.

Index Terms computer-aided creation, virtual pigment, digital technology, creation effect

I. Introduction

Since the 1950s, the birth and development of computers, especially with the addition of Internet applications, has had an extremely profound impact, is changing people's production and life style and mode of thinking at an alarming rate, and driving innovation in the field of art, giving rise to a new form of art, namely digital art. The so-called digital art, also known as digital media art, is a series of design, animation, animation, games and other art-related works produced based on computer processing [1], [2]. And in the dissemination, reproduction, storage and other aspects of the performance of a great advantage, converged into its own unique language paradigm, is a typical result of the integration of modern art and technology development [3]. It is based on the diverse forms of expression of digital art, giving the audience a strong visual impact enjoyment, expressed through graphics, images, software technology, provides a broader creative space, meets the audience's personalized aesthetic needs, helps to cause their emotional resonance [4], [5].

In addition, digital art also has the characteristics of innovation, interactivity and fun [6]. Among them, the interaction mode of digital art is divided into two kinds of visual interaction and behavioral interaction, and the application of artificial intelligence technology adds to its charming color, which produces an immersive feeling through some kind of equipment that brings people stimulation and feedback like touching physical objects [7], [8]. From the dimension of the discipline, digital art is a representative cross-discipline, including the use of technology, art, communication, media and other aspects of the use of knowledge, in the form of expression and dissemination of the form of a strong dependence on digital media technology, highlighting its essence [9]. Under the ecology of the macro-informatization era, digital, as the most typical symbol, leads the trend of innovation and brings many possibilities [10]. The implantation in the field of art, so that it bursts out a unique charm color, but also for the protection of China's intangible cultural heritage and inheritance of innovation to provide a good platform to support, so that it is attached to a strong color of the times, more likely to arouse people's interest, participation in the initiative to significantly enhance [11], [12].

Scholars at home and abroad for the study of digital art, its development can be traced back to the rise of computer art and electronic art in the last century, as early as the 1980s there have been artists began to explore the potential of virtual interactive art and virtual reality technology [13], [14]. From a macro perspective, literature [15] has studied the exploratory and practical aspects of digital art creation with information technology and computer software such as Photoshop, and found that digital art is a creative process driven by the thinking and creativity of human artists. Literature [16] points out in its study that digital art can critically engage with the social history of art by utilizing large datasets and computational methods to discover new insights about the relationship between art, artists and society.

At the micro level, the application of digital art presents a variety of forms, and for the scope of this paper, the focus is on summarizing the relevant research results of digital art in the design of exhibition space. Literature [17] points out that digital art is a reinterpretation of classical art, i.e., the elements are transferred from one system of meaning or artistic discourse to another, supported by digital technology, aiming at a display form that combines art and technology. Literature [18] points out that digital art, in which artists utilize digital technology to interact with nature, can create a new sense of aesthetic and environmental engagement, transforming the art experience from a contemplative to a lived experience. Literature [19] incorporates computational thinking and critical digital production into the spatial design of digital art and points to its importance as a way to equip students with coding skills, expose them to the computational world around them, and explore digital art forms. Literature [20] explores the interaction between computer-aided visual communication technologies and art in new media scenarios, and proposes a new form of digital art based on “intelligent visual art creation” through deep learning.

This paper integrates digital technology into traditional art creation, selects Chinese painting as a research example, and carries out the process of computer-assisted creation of Chinese paintings using color space and visual clustering distance region growth algorithms, intelligent generation models for line drawings, and virtual pigment models for digital paintings based on physical virtualization. In order to obtain the effect of computer-aided creation, the created Chinese paintings were evaluated objectively and subjectively, respectively. The creative effect of this paper's method is examined through the indexes of recall rate, precision rate, LPIPS, FID, PSNR, SSIM and mAP. The subjective evaluation index system is constructed to collect the respondents' perception of the works, and the subjective evaluation results of the computer-aided Chinese painting creation works are calculated and analyzed.

II. Key technologies for computer-assisted drawing

This chapter takes the art of Chinese painting as an example of computer-aided painting.

II. A.Region growing algorithm for color space and visual clustering distance

Region growing algorithm based on color space distance and visual clustering distance is firstly used for interactive color image region segmentation by using image enhancement based on Bezier curve model and after preprocessing the image, simple interactive region growing algorithm is improved.

The judgment of color space distance in region selection is the key, when the R, G, B components of the pixels in the image are small, the RGB color space is used to analyze the image, otherwise the HIS color space is used. Bezier curve image enhancement is used first, and then the distance judgment is based on the following:

(1) RGB color space, Euler distance is used to calculate the color distance, set two different color vectors:

$$C_1 = (r_1, g_1, b_1), C_2 = (r_2, g_2, b_2) \tag{1}$$

Then the color space Euler distance is:

$$D_{Euclidean}(c_1, c_2) = \sqrt{(r_1 - r_2)^2 + (g_1 - g_2)^2 + (b_1 - b_2)^2} \tag{2}$$

The distance criterion for determining that two points belong to the same region is noted as:

$$\begin{aligned} &D_{Euclidean}(c_{seed}, c_{compare}) \le 16; D_{Euclidean}(c_{\exp and}, c_{compare}) \le 8 \\ &D_{Euclidean}(c_{region\_mean}, c_{compare}) \le 10 \end{aligned} \tag{3}$$

In the design, the judgment criteria of homogeneous color can be adjusted according to the quality of the image.

(2) HIS color space, Minkowski distance is used to calculate the color space distance [21], the Minkowski distance of two different color vectors is:

$$d_m(i,j) = \left(\left| h_i - h_j \right|^a + \left| s_i - s_j \right|^b + \left| i_i - i_j \right|^c \right)^{\frac{1}{d}} \tag{4}$$

The distance criterion for determining that two points belong to the same region is noted as:

$$\begin{aligned} &D_m(c_{seed}, c_{compare}) \le 20; D_m(c_{\exp and}, c_{compare}) \le 4 \\ &D_m(c_{region\_mean}, c_{compare}) \le 16 \end{aligned} \tag{5}$$

In the design, the judgment criteria of homogeneous colors can be adjusted according to the quality of the image.

(3) Considering the visual characteristics of the color space, the NBS distance is used to judge the visual dissimilarity of colors, which is calculated as follows:

Set two different color vectors:

$$C_1 = (h_1, i_1, s_1), C_2 = (h_2, i_2, s_2) \tag{6}$$

Then the NBS distance can be calculated as:

$$D_{NBS}(c_1, c_2) = 1.2\left\{2s_1 s_2\left[1 - \cos\left(2p\Delta h / 100\right)\right] + (\Delta s)^2 + (4\Delta i)^2\right\}^{\frac{1}{2}} \tag{7}$$

II. B.Mathematical models related to intelligent generation of line drawings

II. B. 1) A formal representation model for line drawings

(1) Semantic features of national images

Image semantic features depend on specific application domains and user-specific experiential knowledge, in different application domains, people pay attention to different information about images, for the same image features, manifested in different semantic trade-offs, so there is a greater subjectivity and ambiguity about the semantic features, and the totality of all semantic features constitutes the semantic feature space F_s.

Taking Chinese painting as an example, the semantic feature space F_s is defined as:

$$F_s = S_{No} \times S_D \times S_T \tag{8}$$

Among them, S_{No} is the number of the painting, S_D is the dynasty in which it was created, and S_T is the subject.

(2) Shape Characteristics of Chinese Painting Line Drawings

On the basis of the line drawing stroke model and stroke model, the line drawing is generated by combining the line drawing strokes. The XML file is utilized to describe the stroke shape [22], as shown in Figure 1. The utilization of XML format representation is not only beneficial for transmission and storage, but also for transmission to other formats of vectorized formats.

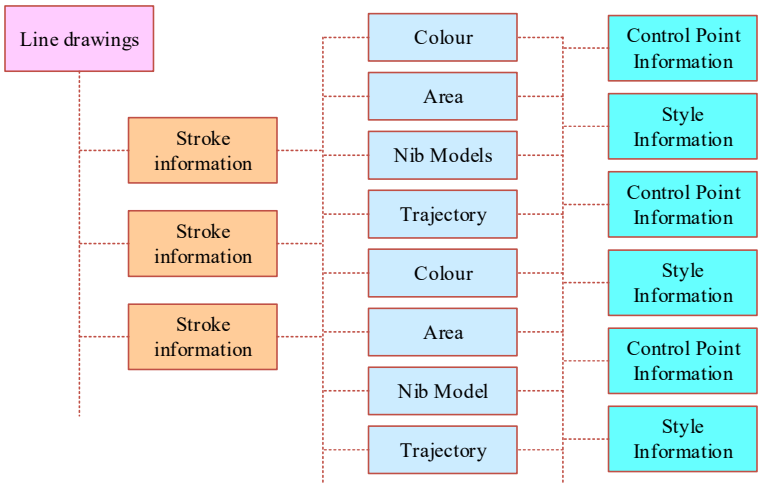

Figure 1: XML graph model

II. B. 2) Mathematical modeling of line drawing strokes

The brushstroke model expresses the thickness and thickness, intensity and lightness styles of Chinese paintings, and the line drawing stroke model is defined in order to express the shape trajectory of Chinese paintings. The line drawing stroke model designed for the purpose of computer-assisted copying of Chinese paintings, since it focuses more on the line shape and thickness of the strokes and has no special requirements for the color and texture characteristics of the strokes, a simple skeleton model based on the splicing of 3-times Bezier curve segments to form the strokes is proposed based on analyzing the work of the predecessors, which consists of the pressure that can respond to the thickness of the strokes parameter F.

The property that the tangent vectors of a Bezier curve at the endpoints fall on the lines connecting the endpoints and neighboring points also makes it relatively easy to splice into first-order continuous curve segments [23]. But to satisfy the first-order continuity between Bezier curve segments it is necessary that the control points P_0' and P_1' in the new segment are on the same line as the control points P_{n-1} and P_n in the previous segment. The P_0'

and P_1' of the new segment of the Bezier curve are on the same line as the P_2 and P_3 of the previous segment of the Bezier curve, and P_0' coincides with P_3.

According to the definition of Bezier curve, a 3 times Bezier curve $P(u)$ can be defined by 4 control points $p_k\left(k=0,\cdots,3\right)$:

$$P(u)=\sum_{k=0}^{3} p_k BEZ_{k,3}(u) \quad 0\le u\le 1 \tag{9}$$

where $BEZ_{k,n}(u)$ is a Bernstein polynomial:

$$BEZ_{k,n}(u)=C_n^k u^k (1-u)^{n-k} \tag{10}$$

Here, $n=3$.

In the implementation, the following data structure is used to record a stroke:

$$L=\left\{w,P_i^3 : i=1,\cdots,n\right\},\ P_i^3=\left\{P_{prev\_i},P_{knot\_i},P_{next\_i}\right\} \tag{11}$$

where w is the width of the stroke, P_{knot_i} is an endpoint of a certain segment of a 3 times Bezier curve, and P_{prev_i} and P_{next_i} are two control points to the left and right of the endpoint P_{knot_i}. Call P_{knot_i} the anchor point and P_{prev_i} and P_{next_i} the control points. This representation can be more intuitive to represent the positional relationship between the control points of each Bezier curve and the strokes. The stroke passes through each anchor point without passing through the control points.

In order to produce line thickness variations when drawing, a set of pressure parameters f is introduced to express the thickness value of the stroke at each anchor point, and the thickness value of the stroke between two neighboring anchors is obtained by interpolating the pressure parameter value linearly at the anchor point.

The stroke after adding the pressure parameter is noted as:

$$L=\left\{w,M_i : i=1,\cdots,n\right\} \tag{12}$$

where w is the width of the stroke.

$$M_i=\{P_i^3,f_i\},\ P_i^3=\{P_{prev\_i},P_{knot\_i},P_{next\_i}\},\ f_i\in[0,1] \tag{13}$$

f_i is the pressure parameter of the stroke at the anchor point P_{knot_i}, and $w\times f_i$ ultimately determines the width of the stroke at that anchor point P_{knot_i}.

II. B. 3) Virtual Brush Model

The establishment of brush model is also an important mathematical model in computer-aided copying, through the brush model can better simulate the texture information of the brush, the intensity of the information.

Through the data package provided by WACOM pressure pen, we can get the pressure information, the direction information of the pressure pen (including the tilt angle of the pressure pen and the pressure plate, the direction angle information of the pressure pen).

The specific calculations are shown below:

Suppose the long and short axes of the ellipse are a and b respectively. The angle of inclination of the pressure pen to the horizontal plane is α, and the pressure at this moment is p, then the maximum width at this moment $w=f(p)$ can be obtained by transforming the long and short axes, respectively:

$$b=w\times\sin(\alpha) \tag{14}$$

$$a=2\times w-b \tag{15}$$

At any moment t, a dynamically varying ellipse can be obtained, which is computed as follows:

$$b(t)=w(t)\times\sin(\alpha(t)) \tag{16}$$

$$a(t)=2\times w(t)-b(t) \tag{17}$$

III. Virtual pigment model for digital painting based on physical virtualization

III. A. Pigment adsorption and desorption between virtual brush and paper surfaces

We have chosen the classical isotherm equation in surface chemical engineering to model the pigment adsorption process. An advantage of this equation is that it models the effect of pressure on the adsorption process:

$$\Delta\rho = \rho e^{-\left(\frac{\kappa_G T}{\beta E_0}\ln\frac{P_{\max}}{P}\right)^2} \tag{18}$$

where ρ is the concentration of pigment particles in the source medium, $\Delta\rho$ is the amount of change in the concentration of the pigment particles that occurs throughout the adsorption process, and κ_G is the gas constant, i.e., $8.314J/(mol\cdot K)$. T is the temperature, which is assumed to be constant at 300 K in this chapter. β is the affinity coefficient, which is used to characterize the degree of polarization of the adsorbed substance. E_0 is the adsorption characteristic energy of the absorber, which depends mainly on the pore density of the absorber, and in this chapter it is assumed to be proportional to the density η of the paper fibers. $P_{\max}$ is the pressure-sensing coefficient of the pigment, and P is the localized pressure in the contact area between the brush and the paper. In the above equation, the term $\ln\frac{P_{\max}}{P}$ is used to reflect the effect of the pressure of the brush in the adsorption process of the pigment mixture solution. The above equation describes an equilibrium state. This is because such an adsorption process usually occurs instantaneously and reaches an equilibrium state. Due to this nature, in order to improve the efficiency of the simulation, we use simple linear scaling when applying the equation, instead of calculating the intermediate simulation results once for each small time interval point. Technical details of the specific linear scaling.

The following equation is applied to ensure the conservation of mass of the pigment particles during adsorption:

$$\left|V_{x,y}^{bru,t}\right|\Delta\rho_{x,y}^{bru,t}(i)+\eta_{x,y}\Delta\rho_{x,y}^{mo,t}(i)=0 \tag{19}$$

where $V_{x,y}^{bru,t}$ denotes the instantaneous local velocity of the point where the surface of the paintbrush comes into contact with the position (x,y) on the paper at the moment t, and $\eta_{x,y}$ is the density of the fibers at the position (x,y) on the paper.

In order to avoid falling into numerical calculation oscillations in simulating the above adsorption process, we introduce an upper limit on the total number of pigment particles that can migrate during the adsorption process. This limit is derived from the following equation:

$$\left|\Delta\rho_{x,y}^{bru,t}(i)\right|+\left|\Delta\rho_{x,y}^{mo,t}(i)\right|=\left|\rho_{x,y}^{bru,t}(i)-\rho_{x,y}^{mo,t}(i)\right| \tag{20}$$

Without loss of generality, we assume that $\rho_{x,y}^{bru,t}(i)>\rho_{x,y}^{mo,t}(i)$. The joint equations (19) and (20), solved, give us the upper limit of $\Delta\rho_{x,y}^{mo,t}(i)$, i.e., $\frac{\left|\rho_{x,y}^{bru,t}(i)-\rho_{x,y}^{mo,t}(i)\right|}{\eta_{x,y}/\left|V_{x,y}^{t}\right|-1}$. Applying this upper bound, we can rewrite (19) as:

$$\tilde{\Delta}\rho_{x,y}^{mo,t}(i)=\min\left(\Delta\rho_{x,y}^{mo,t}(i),\frac{\left|\rho_{x,y}^{bru,t}(i)-\rho_{x,y}^{mo,t}(i)\right|}{\eta_{x,y}/\left|V_{x,y}^{t}\right|-1}\right) \tag{21}$$

We further considered the scenario where there are multiple pigments participating in the adsorption process together and influencing each other, and modeled the process as:

$$\tilde{\tilde{\Delta}}\rho_{x,y}^{mo,t}(i)=\kappa_{mutual}\tilde{\Delta}\rho_{x,y}^{mo,t}(i)+\left(1-\kappa_{mutual}\right)\frac{\sum_{j=1,j\neq i}^{\xi}\tilde{\Delta}\rho_{x,y}^{mo,t}(j)}{\xi-1} \tag{22}$$

Here κ_{mutual} is the coefficient of influence associated with the adsorption of different kinds of pigment particles in the pigment mixture solution. Once the value of $\tilde{\tilde{\Delta}}\rho_{x,y}^{mo,t}(i)$ is derived, we can then update the value of $\rho_{x,y}^{bru,t+\Delta t}(i)$

through the relationship provided by Eqn. (19) as $\rho_{x,y}^{bru,t+\Delta t}(i)=\rho_{x,y}^{bru,t}(i)-\frac{\eta_{x,y}}{\left|V_{x,y}^{t}\right|}\tilde{\tilde{\Delta}}\rho_{x,y}^{mo,t}(i)$. Similarly, when $\rho_{x,y}^{bru,t}(i)<\rho_{x,y}^{mo,t}(i)$, a similar approach can be applied to update $\rho_{x,y}^{bru,t+\Delta t}(i)$. The only difference is that in that case we can introduce the values of $\tilde{\Delta}\rho_{x,y}^{bru,t}(i)$ and $\tilde{\tilde{\Delta}}\rho_{x,y}^{bru,t}(i)$ by the system of equations obtained by the conjunction of Eqs. (21) and (22), and no longer the values of $\tilde{\Delta}\rho_{x,y}^{mo,t}(i)$ and $\tilde{\tilde{\Delta}}\rho_{x,y}^{mo,t}(i)$.

Finally, we also considered the influence of the time of occurrence of the adsorption reaction on the results of the adsorption process. Based on considerations of the efficiency of the simulation, we used a simplified treatment to estimate the value of the adsorbed concentration $\tilde{\tilde{\Delta}}\rho$. We model the adsorption rate $v_{sorption}(t)$ as a variable that decays exponentially, which is consistent with the vast majority of adsorption processes in nature. That is, $v_{sorption}(t)$ is tabulated as $v_{sorption}(t)=\kappa_v e^{-t}$, where κ_v is the adsorption rate parameter. Assume that the time required to reach equilibrium is χ, i.e., $\int_0^{\chi}v_{sorption}(t)dt=\tilde{\tilde{\Delta}}\rho$. Now we have the computational relation $\tilde{\tilde{\Delta}}\rho=\min\left(\frac{1-e^{-t}}{1-e^{-\chi}},1\right)\tilde{\Delta}\rho$. Since we are simulating a time step of Δt, replacing the corresponding variables in the equation gives us: $\rho_{x,y}^{mo,t+\Delta t}=\rho_{x,y}^{mo,t}+\tilde{\tilde{\Delta}}\rho_{x,y}^{mo,t}(i)$, where $\tilde{\tilde{\Delta}}\rho(i)=\min\left(\frac{1-e^{-t}}{1-e^{-\chi}},1\right)\tilde{\Delta}\rho(i)$.

III. B. Pigment diffusion process on paper surface

In order to simulate the active behavior of pigments on a porous and water-permeable paper surface, we model it as a material diffusion process. We choose the convective diffusion equation to express this process quantitatively:

$$\frac{\partial\rho}{\partial t}=\kappa_d\nabla^2\rho-V\nabla\rho \tag{23}$$

where ρ is the concentration of pigment particles in the adsorbed solution, κ_d is the diffusion coefficient, and V is the convective velocity of the external convective field at the time of diffusion onset.

We introduce a factor term that captures the anisotropy in the diffusion process, i.e., (24). Thus Eq. (23) is expanded as:

$$\begin{cases}\dfrac{\partial\rho}{\partial t}=\kappa_{d,x,y}^{x}\dfrac{\partial^2\rho}{\partial x^2}+\kappa_{d,x,y}^{y}\dfrac{\partial^2\rho}{\partial y^2}-V\nabla\rho\\ \kappa_{d,x,y}^{x}=\sum_{i=1}^{nfiber(x,y)}\kappa_{d,i}\cos\left(\varphi_{x,y,i}\right)\\ \kappa_{d,x,y}^{y}=\sum_{i=1}^{nfiber(x,y)}\kappa_{d,i}\sin\left(\varphi_{x,y,i}\right)\end{cases} \tag{24}$$

where $\kappa_{d,x,y}^{x}$ and $\kappa_{d,x,y}^{y}$ are the diffusion coefficient components in the x and y directions at the (x,y) position of the paper, respectively. The $\varphi_{x,y,i}$ is the i th dimensional dominant direction of the paper fiber at position (x,y). This direction is generated during the initialization phase when the program starts the simulation. The $\kappa_{d,i}$ is the diffusion coefficient in the corresponding direction. At each position (x,y) of the paper, there may be more than one diffusion direction, and their specific values are determined by the number of fibers $nfiber(x,y)$ at that point.

In order to be more consistent with the physical reality, we use the dynamic diffusion coefficient approach in our simulations. That is, the diffusion coefficient is affected by the fiber structure in addition. When $i\geq 2$, the diffusion coefficient $\kappa_{d,i,x,y}^{t}$ of the pigment in the i at the point (x,y) of the paper also depends on the concentration of the water $\rho_{x,y}^{mo,t}(0)$, the concentration of the gums $\rho_{x,y}^{mo,t}(1)$ and the density of the fibers here $\eta_{x,y}$. Here, the density distribution of the paper fibers is initialized and generated at the stage when the program simulation is just

started, based on scanned photographs of the internal microstructure of real drawing paper. Based on the above analysis, we can correct Eq. (19) as:

$$\begin{cases} \Delta\kappa_{d,i,x,y}^{t} = \kappa_{d,water}\dfrac{\rho_{x,y}^{mo,t}(0)}{\rho_{x,y}^{mo,t}(i)} - \kappa_{d,glue}\dfrac{\rho_{x,y}^{mo,t}(1)}{\rho_{x,y}^{mo,t}(i)} + \kappa_{d,den}\eta_{x,y} \\ \kappa_{d,i,x,y}^{x} = \Delta\kappa_{d,i,x,y}^{t} + \sum_{i=1}^{nfiber(x,y)} \kappa_{d,j}\cos(\varphi_{x,y,i}) \\ \kappa_{d,i,x,y}^{y} = \Delta\kappa_{d,i,x,y}^{t} + \sum_{i=1}^{nfiber(x,y)} \kappa_{d,j}\sin(\varphi_{x,y,i}) \end{cases} \tag{25}$$

where $\kappa_{d,water}$, $\kappa_{d,glue}$ and $\kappa_{d,den}$ are the diffusion coefficient of water, the diffusion coefficient of glue and the paper fiber density, respectively.

III. C. Pigment Diffusion Process on the Brush Tip

Pigment diffusion on the nib of a paintbrush includes diffusion inside the nib of the brush and on the bristles on its surface. The simulation of the diffusion process of pigment particles inside the nib space is discussed in this section.

In the following, we discuss how to simulate the diffusion behavior of pigment particles inside the pen tip. Using the cylindrical coordinate system (r,θ,z), we can express the classical Fick's second law of diffusion as:

$$\begin{aligned} \frac{\partial\rho_{r,\theta,z}}{\partial t} = \frac{1}{r}\frac{\partial}{\partial r}\left(r\kappa_d\frac{\partial\rho_{r,\theta,z}}{\partial r}\right) + \frac{\partial}{\partial\theta}\left(\frac{\kappa_d}{r}\frac{\partial\rho_{r,\theta,z}}{\partial\theta}\right) \\ + \frac{\partial}{\partial z}\left(r\kappa_d\frac{\partial\rho_{r,\theta,z}}{\partial z}\right) \end{aligned} \tag{26}$$

where $\rho_{r,\theta,z}$ is the concentration of pigment particles at the point (r,θ,z) on the pen tip and κ_d is the diffusion coefficient.

Similar to the simulation of the diffusion of pigment particles on the surface of paper in equation (25), we also introduce a variable diffusion coefficient $\kappa_{d,i,r,\theta,z}^{t}$:

$$\begin{aligned} \kappa_{d,i,r,\theta,z}^{t} = \kappa_{d,i}^{t} + \kappa_{d,water}\frac{\rho_{x,y}^{mo,t}(0)}{\rho_{x,y}^{mo,t}(i)} \\ -\kappa_{d,glue}\frac{\rho_{x,y}^{mo,t}(1)}{\rho_{x,y}^{mo,t}(i)} + \kappa_{d,den}\eta_{r,\theta,z} \end{aligned} \tag{27}$$

where $\kappa_{d,i}^{t}$ is the intrinsic diffusion coefficient of the i th pigment, and $\eta_{r,\theta,z}$ is the density of bristles at the point (r,θ,z) on the center axis of the nib cylinder.

IV. Analysis of the effects of computer-assisted painting creation

IV. A. Objective evaluation analysis

In this study, the Scene and People datasets are used as the datasets for the objective evaluation task.The Scene and People datasets are derived from the RoboFlow 100 dataset collection.The Scene dataset is a single-category dataset containing 3052 landscape images, where the training, validation, and test sets contain 2134, 589, and 329 images, respectively. The People dataset is also a single-category target detection dataset containing 2545 people images, where the training, validation and test sets contain 1745, 547 and 253 images, respectively.

Comparing the computer-aided painting method of this paper with other image generation algorithms (VQVAE, MaskGIT, CDM, ADMGU, MDFG, DiffiT, CADS, BigGAN deep, StyleGAN, StackGAN, AttnGAN, MirrorGAN, DM-GAN, DF-GAN). Painting is created based on the existing dataset images so as to validate the creation effect of each algorithm through the metrics such as Recall, Precision, LPIPS, FID, PSNR, SSIM, and mAP.

For the two datasets of Scene and People, this study conducts two groups of experiments respectively, and each group of experiments is repeated three times, and the experimental results are shown in Table 1 and Table 2. From the experimental results in Table 1 and Table 2, it can be found that the recall, precision, mAP, LPIPS, FID, PSNR, and SSIM values of this paper's computer-assisted drawing-based creation model on the Scene dataset are 0.9466,

0.9958, 0.9944, 0.1758, 0.1508, 0.9947, 0.9915, and the recall, precision, mAP, LPIPS, FID, PSNR, SSIM values on the People dataset, the values of recall, precision, mAP, LPIPS, FID, PSNR, and SSIM are 0.9316, 0.9898, 0.9867, 0.1636, 0.1534, 0.9797, and 0.9882, respectively.The recall, precision, mAP, PSNR, and SSIM of the model in this paper are the largest among all the comparative algorithms of all the comparison algorithms, and LPIPS and FID are the minimum of all the methods. It is enough to show that the computer-assisted painting creation method based on this paper has the best effect in terms of objective evaluation indexes.

Table 1: Experiment results in Scene dataset

Method	Recall	Precision	mAP	LPIPS	FID	PSNR	SSIM
VQVAE	0.8918	0.9502	0.8449	0.4975	0.4584	0.9225	0.9091
MaskGIT	0.9132	0.9625	0.9147	0.2573	0.3493	0.8973	0.8995
CDM	0.8598	0.9857	0.9586	0.2885	0.3495	0.8409	0.8483
ADMGU	0.8582	0.8591	0.9663	0.4765	0.1906	0.9232	0.9239
MDFG	0.8416	0.9103	0.8396	0.4273	0.3714	0.8634	0.9317
DiffiT	0.8943	0.9617	0.9588	0.2755	0.3847	0.9068	0.9934
CADS	0.8463	0.8639	0.8846	0.4825	0.3344	0.8561	0.8448
BigGAN deep	0.8314	0.8441	0.8737	0.3063	0.3756	0.8646	0.9243
StyleGAN	0.8519	0.9257	0.8816	0.2433	0.3346	0.8834	0.9485
StackGAN	0.9389	0.9074	0.8713	0.2397	0.2934	0.8159	0.9405
AttnGAN	0.9052	0.9414	0.8643	0.4033	0.3437	0.9387	0.8478
MirrorGAN	0.8466	0.9358	0.9306	0.3649	0.2457	0.8298	0.9477
DM-GAN	0.8856	0.9535	0.9222	0.2313	0.2124	0.9091	0.8413
DF-GAN	0.8301	0.9438	0.8508	0.2166	0.3165	0.8541	0.9157
Ours	0.9466	0.9958	0.9944	0.1758	0.1508	0.9947	0.9915

Table 2: Experiment results in People dataset

Method	Recall	Precision	mAP	LPIPS	FID	PSNR	SSIM
VQVAE	0.8734	0.8839	0.9046	0.2384	0.4551	0.8878	0.9088
MaskGIT	0.9141	0.9243	0.9419	0.3633	0.4279	0.8133	0.9178
CDM	0.9159	0.8943	0.8441	0.3648	0.2467	0.9215	0.9572
ADMGU	0.8994	0.9405	0.8309	0.3159	0.2163	0.8283	0.8835
MDFG	0.8337	0.9188	0.8612	0.2422	0.4755	0.8625	0.9084
DiffiT	0.8437	0.8305	0.8719	0.3515	0.2738	0.9047	0.9736
CADS	0.9153	0.8369	0.8743	0.2781	0.4838	0.9016	0.8782
BigGAN deep	0.8082	0.9589	0.9138	0.3145	0.4733	0.8839	0.8627
StyleGAN	0.8601	0.9603	0.8992	0.2935	0.3969	0.9691	0.9757
StackGAN	0.8715	0.8549	0.8666	0.3973	0.2368	0.8198	0.8678
AttnGAN	0.9016	0.9199	0.8271	0.2996	0.4536	0.8174	0.9508
MirrorGAN	0.8516	0.8912	0.9152	0.4485	0.3896	0.9082	0.8468
DM-GAN	0.8337	0.9371	0.9259	0.4003	0.2614	0.9311	0.8784
DF-GAN	0.8753	0.9203	0.9621	0.2031	0.4567	0.9611	0.8379
Ours	0.9316	0.9898	0.9867	0.1636	0.1534	0.9797	0.9882

IV. B. Subjective evaluation analysis

IV. B. 1) Construction of subjective evaluation index system

This paper invites 10 relevant experts to make suggestions for the subjective evaluation index system of computer-aided creation, adopts the hierarchical analysis method for subjective evaluation of the effect of computer-aided creation, still takes Chinese painting as an example, and constructs the subjective evaluation index system of computer-aided creation of Chinese painting as shown in Table 3.

Indicator weights reflect the degree of importance of an indicator, and indicators with larger weight values have a greater impact on the evaluation results. The expert advisory group for weighting construction is still composed of the expert advisory group (10 people) established in the construction of the indicator system. The experts need to feedback the following opinions through the questionnaire:

(1) Score the importance of the 7 level 1 indicators (using a 10-point scale).

Table 3: Subjective evaluation index system for computer aided Chinese painting creation

Target layer	Primary index	Second index
Subjective evaluation for computer aided Chinese painting creation	Integrity (A1)	Fully visible image (A11)
		Content integrity (A12)
		Theme integrity (A13)
	Equalization (A2)	Main body center (A21)
		Proportional equilibrium (A22)
		Image correction (A23)
		Content coverage (A24)
		Effective occupancy ratio (A25)
	Brightness (A3)	Image shading (A31)
		Feature visibility (A32)
		Brightness uniformity (A33)
		Detail identification (A34)
	Color (A4)	No color distortion (A41)
		Color identification (A42)
		Color uniformity (A43)
		Color coordination (A44)
	Resolution (A5)	Content clarity (A51)
		Detail clarity (A52)
		Low image noise (A53)
		Low image jamming (A54)

Table 4: Subjective evaluation index weight for computer aided Chinese painting creation

Target layer	Primary index	Weight	Second index	Weight
Subjective evaluation for computer aided Chinese painting creation	Integrity (A1)	0.1753	Image visibility (A11)	0.3486
			Content integrity (A12)	0.3312
			Theme integrity (A13)	0.3202
	Equalization (A2)	0.2243	Main body center (A21)	0.1853
			Proportional equilibrium (A22)	0.2074
			Image correction (A23)	0.1988
			Content coverage (A24)	0.2139
			Effective occupancy ratio (A25)	0.1946
	Brightness (A3)	0.2014	Image shading (A31)	0.2435
			Feature visibility (A32)	0.2568
			Brightness uniformity (A33)	0.2482
			Detail identification (A34)	0.2515
	Color (A4)	0.2106	No color distortion (A41)	0.2612
			Color identification (A42)	0.2175
			Color uniformity (A43)	0.2536
			Color coordination (A44)	0.2677
	Resolution (A5)	0.1884	Content clarity (A51)	0.2724
			Detail clarity (A52)	0.2718
			Low image noise (A53)	0.2233
			Low image jamming (A54)	0.2325

(2) Score the importance of a number of secondary indicators under each primary indicator (using a 3-point scale: low, medium, and high).

After collecting the feedback data from the expert group, the weights were calculated using the preferential order diagram method. When calculating the weights by the preferential order diagram method, the average size of each score was compared two by two, with the item with the larger average value being scored as 1, the smaller one as 0, and both items being scored as 0.5 when the average values were equal. Subsequently, the scores of the indicators in the weight table of the superiority chart are added together, and then do the normalization process,

after the processing of the superiority chart method, the larger the average value means that the importance of the higher, the higher the weight will also be. The weight value of each indicator is obtained as shown in Table v.

IV. B. 2) Subjective evaluation results

Utilizing the key foundation of computer-aided painting and the painting model described in this paper for the creation of Chinese paintings, a questionnaire is designed and distributed for the created Chinese paintings according to the above subjective evaluation index system of computer-aided Chinese painting creation. A total of 1,000 questionnaires were distributed and 896 were recovered, with a recovery rate of 89.6%, of which 874 were valid questionnaires, with a questionnaire validity rate of 87.4%. A five-point Likert scale was used as the basis for calculating the scores, in which 1, 2, 3, 4, and 5 indicate very poor, poor, fair, good, and very good, respectively. According to the subjective evaluation indexes of computer-assisted Chinese painting creation developed in this study, the corresponding scores were determined, and the results of subjective evaluation are shown in Table 5.

From the results in Table 5, the respondents hold a better view of the Chinese painting works created through the computer-aided creation method in this paper. The scores of the first-level indicators are distributed around 4.30, of which completeness, balance, brightness, color, and resolution obtain 4.32, 4.39, 4.277, 4.32, and 4.40 respectively. The subjective evaluation scores of the secondary indicators fall within the interval of [4.15, 4.56], and the secondary indicator that receives the best subjective evaluation is content clarity, and the secondary indicator with the lowest score is color uniformity. Overall, the subjective evaluation score of computer-assisted Chinese painting creation is 4.34, which is at a good level.

Table 5: Subjective evaluation results for computer aided Chinese painting creation

Target layer	Primary index	Score	Second index	Score
Subjective evaluation for computer aided Chinese painting creation (4.34)	Integrity (A1)	4.32	Image visibility (A11)	4.28
			Content integrity (A12)	4.23
			Theme integrity (A13)	4.47
	Equalization (A2)	4.39	Main body center (A21)	4.27
			Proportional equilibrium (A22)	4.54
			Image correction (A23)	4.36
			Content coverage (A24)	4.33
			Effective occupancy ratio (A25)	4.43
	Brightness (A3)	4.27	Image shading (A31)	4.39
			Feature visibility (A32)	4.17
			Brightness uniformity (A33)	4.17
			Detail identification (A34)	4.34
	Color (A4)	4.32	No color distortion (A41)	4.33
			Color identification (A42)	4.33
			Color uniformity (A43)	4.15
			Color coordination (A44)	4.45
	Resolution (A5)	4.40	Content clarity (A51)	4.56
			Detail clarity (A52)	4.18
			Low image noise (A53)	4.42
			Low image jamming (A54)	4.46

V. Conclusion

The article takes the art of painting as an example to create traditional Chinese paintings with the help of computer-aided creative techniques such as area growth algorithms, intelligent generation models for line drawings, and virtual pigment models for digital paintings, and conducts both objective and subjective evaluations of the produced paintings.

(1) On both Scene and People datasets, this paper's model achieves the best objective evaluation results. The recall, precision, mAP, PSNR, and SSIM values of this paper's model on the Scene dataset are 0.9466, 0.9958, 0.9944, 0.9947, and 0.9915, respectively, and on the People dataset are 0.9316, 0.9898, 0.9867, 0.9797, and 0.9882, respectively, which are the maximum values of all methods in the maximum value, and 0.1758 and 0.1508 for LPIPS and FID on the Scene dataset, and 0.1636 and 0.1534 on the People dataset, respectively, all of which are the minimum values.

(2) In the subjective evaluation results, the overall subjective evaluation of the Chinese painting works created by utilizing the method of this paper is 4.34 points, with the score of the first-level indexes ranging from 4.27 to 4.40, and the score of the second-level indexes are not less than 4.15 points, which obtains a better subjective evaluation result.

References

[1] Tang, B., & Ge, C. (2021). Application of Computer Software Technology in Art and Technology Creation. World Scientific Research Journal, 7(6), 356-363.

[2] Harbinja, E. (2019). Inheritance of digital media. Partners for Preservation: Advancing digital preservation through cross-community collaboration, 1.

[3] Zhou, K., Wang, K., & Lin, X. (2021). Research on the inheritance and protection of folk art and culture from the perspective of network cultural governance. Plos one, 16(2), e0246404.

[4] Yuying, Y. (2023). Research on the Application of New Media Technology in the Digital Inheritance of Cantonese Opera Art. Media and Communication Research, 4(6), 19-23.

[5] Deng, J. (2023). A brief analysis of the path of intangible cultural heritage inheritance and innovative development under digital technology. Journal of Innovation and Development, 3(3), 29-32.

[6] Wang, L. (2023, December). Digital Technology in Promoting Stakeholders Transforming in Cultural Inheritance. In 2023 16th International Symposium on Computational Intelligence and Design (ISCID) (pp. 165-168). IEEE.

[7] Tan, Z. (2023). Digital inheritance and innovation of art and culture based on vr technology. cultural heritage, 4, 5.

[8] Arora, P., & Vermeylen, F. (2013). The end of the art connoisseur? Experts and knowledge production in the visual arts in the digital age. Information, Communication & Society, 16(2), 194-214.

[9] Avila, L., & Bailey, M. (2016). Art in the digital age. IEEE Computer Graphics and Applications, 36(04), 6-7.

[10] Yiguang, L. (2024). Cultural inheritance and media communication of national costumes in digital age. Academic Journal of Humanities & Social Sciences, 7(4), 73-77.

[11] Liu, Y. (2022). Application of digital technology in intangible cultural heritage protection. Mobile Information Systems, 2022(1), 7471121.

[12] Liu, J. (2022). Digitally Protecting and Disseminating the Intangible Cultural Heritage in Information Technology Era. Mobile Information Systems, 2022(1), 1115655.

[13] Ahmed, S. U. (2018, June). Interaction and interactivity: In the context of digital interactive art installation. In International Conference on Human-Computer Interaction (pp. 241-257). Cham: Springer International Publishing.

[14] Ruan, Y. (2022). Application of immersive virtual reality interactive technology in art design teaching. Computational intelligence and neuroscience, 2022(1), 5987191.

[15] Mohsin, S. (2021). Iraqi digital art: origin and evolution. Iraqi Journal of Science, 191-197.

[16] Jaskot, P. B. (2019). Digital art history as the social history of art: Towards the disciplinary relevance of digital methods. Visual Resources, 35(1-2), 21-33.

[17] Jevtić, M., & Tomc, H. G. (2018). the reinterpretation of classical art in digital format. Journal of Graphic Engineering and Design, 9(2), 5-15.

[18] Coles, L. L., & Pasquier, P. (2015). Digital eco-art: Transformative possibilities. Digital Creativity, 26(1), 3-15.

[19] Knochel, A. D., & Patton, R. M. (2015). If art education then critical digital making: Computational thinking and creative code. Studies in Art Education, 57(1), 21-38.

[20] Wang, R. (2021). Computer-aided interaction of visual communication technology and art in new media scenes. Computer-Aided Design and Applications, 19(S3), 75-84.

[21] Mahinda Mailagaha Kumbure & Pasi Luukka. (2024). Local means-based fuzzy k-nearest neighbor classifier with Minkowski distance and relevance-complementarity feature weighting. Granular Computing,9(4),73-73.

[22] S. Tharun Reddy,Tharun Reddy S.,Mothe Rajesh,Ghate Sukhaveerji & Sunil G. (2020). Evaluation and scrutiny of XML files, XML empowered records and native XML records. IOP Conference Series: Materials Science and Engineering,981(2),022074-.

[23] Gaoyang Xie,Liqing Fang,Xujun Su,Deqing Guo,Ziyuan Qi,Yanan Li & Jinli Che. (2025). Research on Risk Avoidance Path Planning for Unmanned Vehicle Based on Genetic Algorithm and Bezier Curve. Drones,9(2),126-126.